Spectroscopic Characterization of 4′-Substituted Aromatic Self-Assembled Monolayers on GaAs(100) Surface

A. Shaporenko,[†] K. Adlkofer,[‡] L. S. O. Johansson,[§] A. Ulman,[||] M. Grunze,[†] M. Tanaka,[‡] and M. Zharnikov*,[†]

Angewandte Physikalische Chemie, Universität Heidelberg, Im Neuenheimer Feld 253, D-69120 Heidelberg, Germany, Lehrstuhl für Biophysik E22, Technische Universität München, James-Franck-Strasse, D-85748, Garching, Germany, Department of Physics, Karlstad University, Universitetsgatan 1, S-65188 Karlstad, Sweden, and Department of Chemistry and the NSF MRSEC for Polymers at Engineered Interfaces, Polytechnic University, Brooklyn, New York 11201

Received: June 30, 2004; In Final Form: August 26, 2004

High-resolution X-ray photoelectron spectroscopy and near-edge X-ray absorption fine structure spectroscopy were applied to characterize GaAs(100) surface engineered by self-assembled monolayers (SAMs) of 4′-substituted aromatic molecules: 4′-methyl-4-mercaptobiphenyl (CH_3−BPT) and 4′-hydroxy-4-mercaptobiphenyl (OH−BPT). Both of these molecules formed ordered and densely packed SAMs on GaAs, which were able to protect the substrate from degradation under ambient conditions. The molecular attachment in the SAMs is mediated by As-thiolate bond while the intact aromatic backbones have an upright orientation with average tilt angles of 31.0° and 37.2° for CH_3−BPT and OH−BPT films, respectively. The difference in the tilt angle is attributed to a higher (by 7−10%) packing density of the former SAM, suggesting that the character of 4′-substitution affects the quality of the resulting SAM on the GaAs substrate.

1. Introduction

The fabrication of functional interfaces and links between biological objects and versatile substrates is an important issue from the viewpoint of both basic research and applications. Among the relevant materials, GaAs, which enables flexible band gap engineering, is quite promising for the fabrication of nanostructure devices (such as two-dimensional electron gases, high electron mobility transistors, etc),[1,2] which can be further integrated with biofunctional molecular systems. There are, however, some constrains in application of GaAs-based systems in life science. One of the most serious issues is chemical instability of the respective surface both under ambient conditions and in physiological electrolytes. A way to protect this surface is its functionalization with self-assembled monolayers (SAMs), which are ordered 2D-assembles of chemisorbed molecules consisting of three essential parts: headgroup, molecular spacer, and a tailgroup.[3] So far, most attention has been paid to SAMs of alkylthiolates (AT),[4−11] which resulted in the stabilization of the GaAs/electrolyte interface in a physiological buffer for more than 24 h[10,11] and a significant enhancement in photoluminescence yield from the InAs quantum dots with thin GaAs cap layers.[12,13]

Recently, we extended the range of thiol-derived compounds used for the functionalization of the GaAs surface and tried a molecule with a rigid aromatic backbone, namely, a nonsubstituted aromatic thiol 1,1′-biphenyl-4-thiol (BPT).[14,15] BPT molecules form well-ordered and densely packed SAMs on GaAs(100), and such films prevent an oxidation and contamination of the substrate, keeping the GaAs surface in a pristine state.[14,15] In addition, we have shown that the presence of the BPT monolayer significantly suppresses charge transfer at the GaAs/electrolyte interface at neutral pH conditions and stabilizes this interface.[14] More recently, this strategy has been transferred onto two-dimensional electron gas (2DEG) near the GaAs surface.[16] BPT monolayers effectively stabilized the sheet resistance in the 2DEG layer for several hours, suggesting a large potential as a surface-sensitive liquid-phase chemical sensor.

A further step was to attach a functional tailgroup to the BPT backbone, which allows one to have a control over the wetting properties of the GaAs surface, in addition to its protection from oxidation and degradation. Within this approach, stable chemical engineering of stoichiometric GaAs(100) surfaces was recently achieved by deposition of two types of functionalized aromatic molecules: 4′-methyl-4-mercaptobiphenyl (CH_3−BPT) and 4′-hydroxy-4-mercaptobiphenyl (OH−BPT).[17] Such a functionalization renders the GaAs surface hydrophobic and hydrophilic, respectively, and both monolayer types are quite stable, even in electrochemical electrolytes.

In this paper, we perform a detailed spectroscopic analysis of SAMs formed from CH_3−BPT (CH_3−$(C_6H_4)_2$−SH) and OH−BPT (HO−$(C_6H_4)_2$−SH) on stoichiometric GaAs(100) surfaces. For this purpose, we applied two highly sensitive and chemically specific experimental techniques: synchrotron-based high-resolution X-ray photoelectron spectroscopy (HRXPS) and near-edge X-ray absorption fine structure (NEXAFS) spectroscopy. They provide complementary information on chemical identity of the CH_3−BPT and OH−BPT films and the film/GaAs interface as well as give an insight into the film structure.

In the next section, we describe the experimental procedure and techniques, which is followed by presentation and discussion

* Corresponding author. Tel: +49−6221−544921; fax: +49−6221−546199; e-mail: Michael.Zharnikov@urz.uni-heidelberg.de.
[†] Universität Heidelberg.
[‡] Technische Universität München.
[§] Karlstad University.
[||] Polytechnic University.

10.1021/jp040474a CCC: $27.50
Published on Web 10/23/2004

of the experimental data in sections 3 and 4, respectively. Finally, the results are summarized in section 5.

2. Experimental Section

The substrate was an undoped GaAs layer with a thickness of 1000 Å, which was epitaxially grown on the surface of single crystalline *n*-type GaAs(100) wafers doped with $(2.2-3.4) \times 10^{18}$ cm^{-3} Si (American Xtal Technology Inc., Fremond, CA). Synthesis of 4′-substituted-4-mercaptobiphenyls was reported elsewhere.[18] All other chemicals were purchased from Aldrich (Steinheim, Germany) and used without further purification.

The deposition of SAMs was carried out under nitrogen (N_2) atmosphere to reduce surface oxidation. Prior to the SAM fabrication, the samples were sonicated in acetone for 3 min and rinsed intensively with ethanol. After this pretreatment, native oxide of GaAs was removed by etching the sample in concentrated HCl for 1 min. These freshly etched substrates were immediately immersed into 0.1 mM solution of CH_3-BPT or OH−BPT in dry ethanol and kept there at 50 °C for 20 h.[14] After the SAM formation, the samples were taken out from the reactor, briefly sonicated in ethanol, dried by a N_2 flow, and put into a N_2-filled vial until the spectroscopic characterization.

The characterization was performed at room temperature and a base pressure lower than 1.5×10^{-9} Torr. The spectra acquisition time was selected in such a way that no noticeable X-ray damage was observed during the spectra collection.[19−22]

The HRXPS measurements were carried out at the D1011 beamline of the synchrotron storage ring MAX II at MAX-Lab in Lund, Sweden. The spectra (Ga 3d, As 3d, C 1s, O 1s, and S 2p) were collected by a SCIENTA analyzer in normal emission geometry. Excitation energies in the range of 130−600 eV were used. The choice of photon energy (PE) for a particular spectrum was based on the optimization of the photoionization cross section for the corresponding core level[23−25] and on adjustment of either surface or bulk sensitivity.

The energy resolution was better than 100 meV, allowing a clear separation of individual spectral components. The energy width of the individual emissions was close to the intrinsic energy spread of the respective core-level photoemission process. Energy calibration was performed individually for every spectrum to avoid effects related to the instability of the monochromator. The energy scale was referenced to the pronounced Au $4f_{7/2}$ "bulk" peak (83.93 eV) of a reference C12/Au sample,[21,26] which was attached to the same sample holder as the probed one. The value of 83.93 eV was derived from an independent calibration to the Fermi edge of a clean Pt-foil. It is quite close to a value of 83.95 eV given for Au $4f_{7/2}$ by the latest ISO standard.[27]

The decomposition of the HRXPS spectra was performed self-consistently over the entire data set. The spectra were fitted using Voigt peak profiles and a Shirley background. To fit the doublet emissions (Ga 3d, As 3d, and S 2p), we used two peaks with the same full width at half-maximum (fwhm), a reasonable spin−orbit splitting, and branching ratios of 2:1 ($2p_{3/2}/2p_{1/2}$) and 3:2 ($3d_{5/2}/3d_{3/2}$). Because of the ultimate energy resolution and the presence of the spectra dominated by a single doublet, we were able to derive the initial setting for the respective parameters directly from the spectra. The resulting accuracy of the binding energies (BE) and fwhm's reported here is 0.04−0.05 eV. These values are noticeably lower than the ultimate accuracy of the experimental setup (see, e.g., ref 28), but mostly reflect the distribution of the resulting fit parameters over the spectra of different samples.

The NEXAFS spectroscopy measurements were performed at the HE-SGM beamline of the synchrotron storage ring BESSY II in Berlin, Germany. The spectra acquisition was carried out at the C K-edge in the partial electron yield mode with a retarding voltage of −150 V. Linear polarized synchrotron light with a polarization factor of ≈82% was used. The energy resolution was ≈0.40 eV. The incidence angle of the light was varied from 90° (**E**-vector in surface plane) to 20° (**E**-vector near surface normal) in steps of 10−20° to monitor the orientational order within the molecular films. This approach is based on so-called linear dichroism in X-ray absorption, that is, the strong dependence of the cross section of the resonant photoexcitation process on the orientation of the electric field vector of the linearly polarized light with respect to the molecular orbital of interest.[29] The raw NEXAFS spectra were normalized to the incident photon flux by division through a spectrum of a clean, freshly sputtered gold sample. Before the normalization, a spectrum of freshly etched GaAs was subtracted from the raw spectrum of the CH_3-BPT- or OH−BPT-coated GaAs.[30,31] The energy scale was referenced to the pronounced π_1^* resonance of highly oriented pyrolytic graphite at 285.38 eV.[32]

3. Results

3.1 HRXPS Characterization. As a reference to the deposited CH_3-BPT and OH−BPT films, we studied several samples of bare GaAs(100) substrate, namely, (i) as-prepared GaAs, (ii) freshly etched GaAs, and (iii) freshly etched GaAs stored in N_2 under the same conditions as the BPT-coated wafers. The samples i were just cleaned in acetone and ethanol, as mentioned in Section 2 while the samples ii were etched by HCl directly at the synchrotron and put in the load-lock chamber of the experimental station immediately after the etching and rinsing by water.

The Ga 3d and As 3d HRXPS spectra of the GaAs samples are presented in Figure 1. These spectra were acquired at a photon energy of 130 eV, which was specially chosen to achieve a maximum surface sensitivity (the electron mean free path reaches its minimum value at kinetic energies of 50−100 eV).[33,34] The spectra are decomposed into individual spectral components. The derived parameters and the assignments of individual peaks are presented in Table 1, except for the broad maxima related to Ga and As oxides, which were not considered in detail. Though technically possible, any fitting of broad, structureless features by a variety of narrow peaks or doublets is rather arbitrary.

The spectra of the as-prepared GaAs in the upper panels of Figure 1 show that the entire near-surface region of this sample is heavily oxidized. Both Ga 3d and As 3d spectra are dominated by the emissions associated with Ga and As oxides. The emissions assigned to stoichiometric GaAs (light gray) and elemental arsenide (gray) at the sample surface are rather weak. Most of the oxides can be, however, removed by the wet chemical etching, as follows from the spectra of the respective sample in the middle panels of Figure 1. These spectra are dominated by the emissions related to stoichiometric GaAs (light gray) and elemental arsenide **(**gray**)**. The oxide-related features constitute only ≈20% of the total intensity.

Upon a prolonged exposure of the etched sample to ambient, the extent of oxidation and contamination progressively increases, so that the entire presurface region becomes oxidized again and the spectra change toward those for the as-prepared sample. Even a careful handling and the sample storage under N_2 (for several days) could not prevent the surface degradation,

TABLE 1: Parameters of the Individual Emissions in the Ga 3d and As 3d Spectra in Figures 1−3[a]

	binding energy (eV)	assignment	fwhm (eV)	spin−orbit splitting (eV)	branching ratio
Ga $3d_{5/2}$	19.20 ± 0.04	GaAs	0.51 ± 0.04	0.43	3/2
	19.8 ± 0.1	Ga_2O_3 or the surface Ga 3d component			
	>19.8	Ga oxides			
As $3d_{5/2}$	41.05 ± 0.03	GaAs	0.60 ± 0.05	0.69	3/2
	41.72 ± 0.05	elementary As (As^0)			
	42.14 ± 0.05	As−S			
	>43.0	As oxides			

[a] The parameters were derived from the self-consistent fitting procedure. The error bars reflect the scattering of the fitting parameters between the spectra for different samples and different PEs. The assignments were performed in accordance with refs 11, 15, and 35−41.

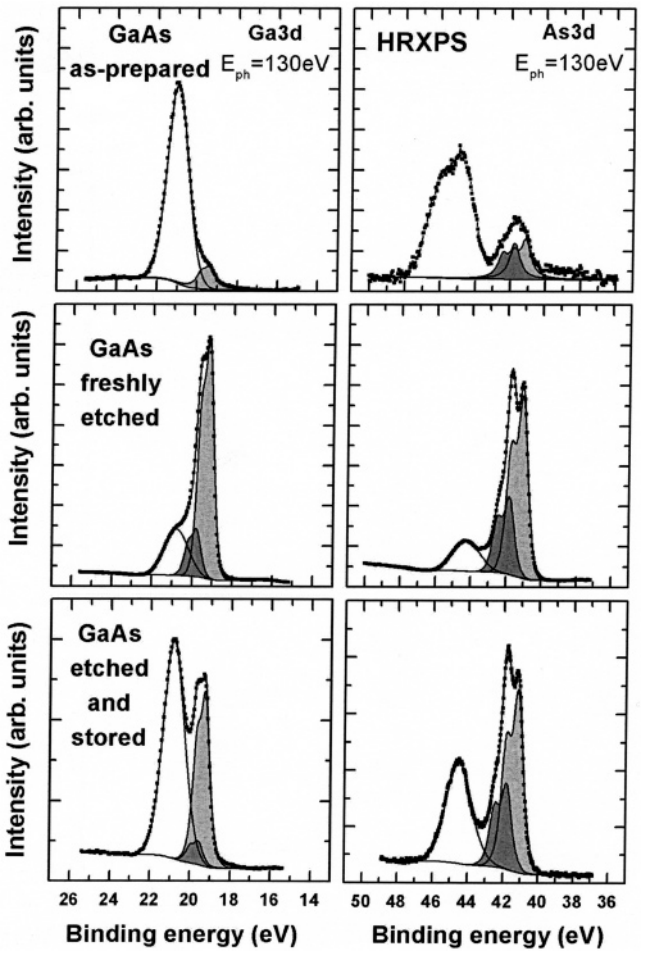

Figure 1. Ga 3d and As 3d HRXPS spectra of as-prepared (upper panels), freshly etched (middle panels), and N_2-stored after etching (bottom panels) bare GaAs (see text for details). The spectra were acquired at a PE of 130 eV. A decomposition of distinct spectral features by doublets related to individual chemical species is shown. Ga 3d spectra: light gray, GaAs; gray, a Ga oxide or the surface Ga 3d component; As 3d spectra: light gray, GaAs; gray, elementary As. The broad peaks at the high-binding energy side of the shadowed doublets correspond to Ga and As oxides.

as follows from the spectra of the respective sample in the bottom panels of Figure 1, in which the oxide-related emissions are much more intense than those in the spectra of the freshly etched sample. According to the former spectra, 62% of the Ga atoms and 37% of the As atoms at the surface of freshly etched GaAs substrate become oxidized after a prolonged storage, even though special care was taken to avoid a direct exposure of the sample to ambient.

The spectra of freshly etched and N_2-stored GaAs can be considered as direct references for the BPT-coated samples. The former spectra are coarsely representative for the state of the GaAs substrate immersed into the BPT solution while the latter spectra describe the degradation of a bare substrate kept at the same conditions as the BPT-coated samples.

The Ga 3d and As 3d HRXPS spectra of CH_3−BPT- and OH−BPT-coated GaAs are presented in Figures 2 and 3, respectively. These spectra were acquired at photon energies of 130 eV (upper panels) and 600 eV (bottom panels) to monitor the changes in the intensity of the individual spectral components by going from the sample surface to its bulk. At these photon energies, the effective sampling depth ($\approx 3\lambda$) is about 18 Å (130 eV) and 33 Å (600 eV),[33,34] with a larger spectral weight for the contributions from the topmost layers. In the same manner as the spectra in Figure 1, the spectra in Figures 2 and 3 are decomposed into individual spectral components, with the parameters and assignments given in Table 1.

A comparison of the spectra in Figures 2 and 3 with those in Figure 1 clearly demonstrates that the CH_3−BPT and OH−BPT films protect the underlying GaAs substrate from oxidation and degradation: the surface-sensitive spectra (130 eV) of the BPT-coated GaAs are similar to those of freshly etched GaAs (Figure 1, middle panels) and are dominated by the emissions related to the stoichiometric GaAs (light gray) and elemental As (gray). The spectral weight of the former emissions increases even further by going to 600 eV (bottom panels in Figures 2 and 3), which suggests that both elemental As and residual Ga and As oxides are located at the substrate surface (i.e., at the SAM−GaAs interface).

In addition to the abovementioned emissions, a new doublet **(**black**)** assigned to As bonded to the thiol headgroup of CH_3−BPT or OH−BPT is also observed at 42.14 eV. In accordance with the expectations, the intensity of this doublet decreases with increasing sampling depth, as follows from the comparison of the 130 and 600 eV spectra in Figures 2 and 3.

The formation of the As-thiolate bond is also exhibited in the S 2p spectra of CH_3−BPT- and OH−BPT-coated GaAs, presented in Figure 4 along with the C 1s and O 1s spectra and the data for the N_2-stored, bare GaAs substrate. In the S 2p spectra, a single doublet at a characteristic binding energy of 162.6 eV (S $2p_{3/2}$) is observed. Interestingly, this energy is somewhat higher than that for the thiol-derived SAMs on noble metal substrates (162.0 eV),[26,42−44] which is presumably related to the screening of the photoemission hole by the substrate electrons in the metal. In addition to the thiolate-related doublet, there are also minor contributions from "disulfide" species at 163.7 eV[44] and Ga 3s states at 161.6 eV.[41] The latter emission is also observed in the S 2p spectra of the N_2-stored, bare GaAs substrate.

The conclusions derived from the Ga 3d, As 3d, and S 2p data are supported by the respective C 1s and O 1s spectra. The C 1s spectra in Figure 4 exhibit a characteristic signature of aromatic SAMs—a main emission at 284.65 eV and a shake-up shoulder at high binding energy (286.5 eV).[26,44] In the OH−BPT, there is also an additional shoulder at 286.3 eV, which is related to the hydroxy group. The corresponding feature is also observed in the O 1s spectra of the OH−BPT-coated GaAs, at

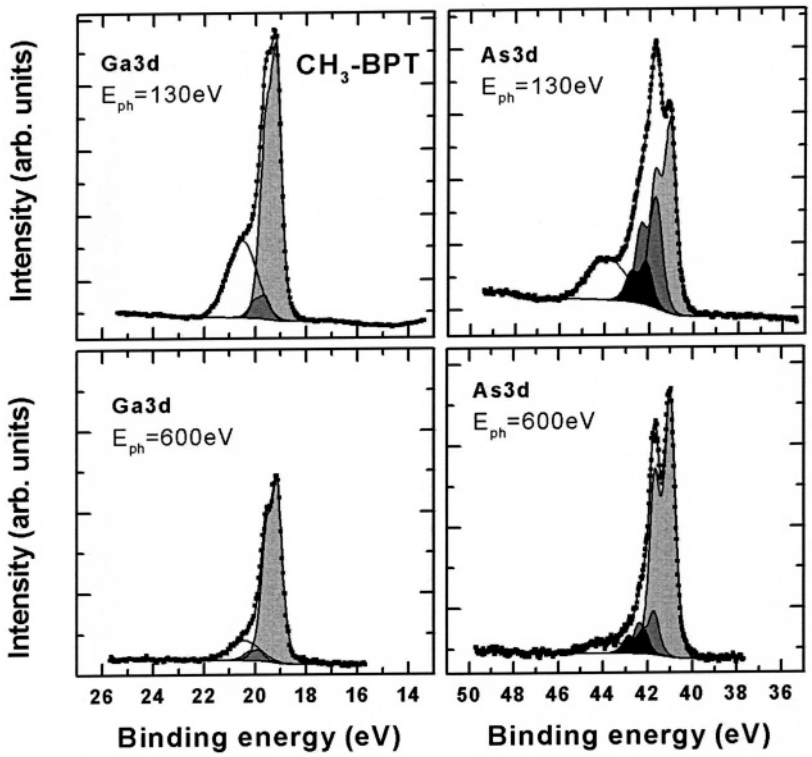

Figure 2. Ga 3d and As 3d HRXPS spectra of CH_3−BPT-coated GaAs. The spectra were acquired at PEs of 130 eV (upper panels) and 600 eV (bottom panels) and are dominated by contributions from the sample surface and bulk, respectively. A decomposition of distinct spectral features by doublets related to individual chemical species is shown. Ga 3d spectra: light gray, GaAs; gray, a Ga oxide or the surface Ga 3d component; As 3d spectra: light gray, GaAs; gray, elementary As; black, S−As. The shoulders at the high-binding energy side of the shadowed doublets correspond to Ga and As oxides.

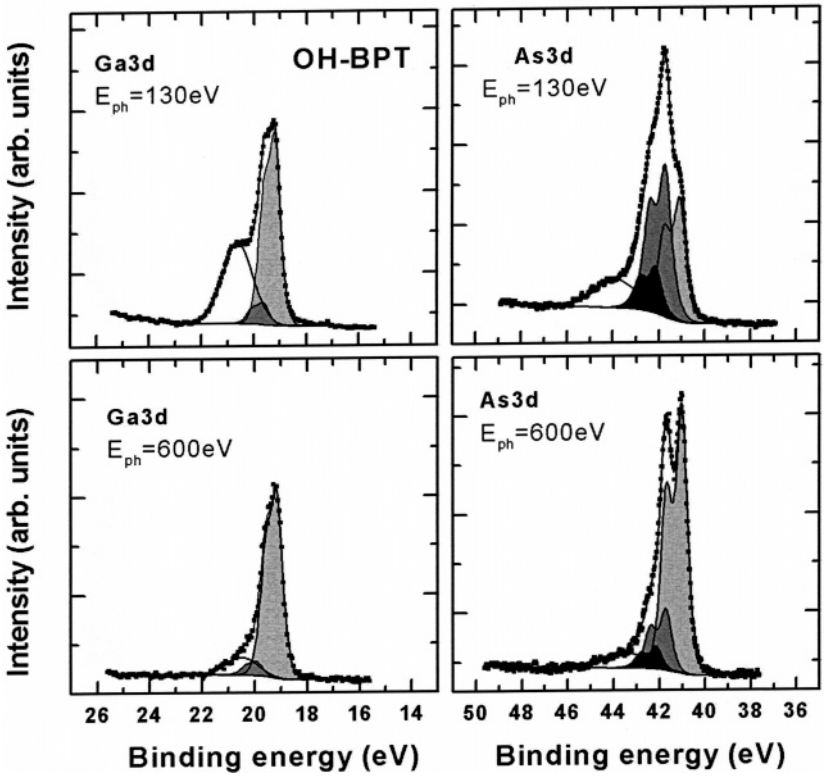

Figure 3. Ga 3d and As 3d HRXPS spectra of OH−BPT-coated GaAs. The spectra were acquired at PEs of 130 eV (upper panels) and 600 eV (bottom panels) and are dominated by contributions from the sample surface and bulk, respectively. A decomposition of distinct spectral features by doublets related to individual chemical species is shown. Ga 3d spectra: light gray, GaAs; gray, a Ga oxide or the surface Ga 3d component; As 3d spectra: light gray, GaAs; gray, elementary As; black, S−As. The shoulders at the high-binding energy side of the shadowed doublets correspond to Ga and As oxides.

533.0 eV. In addition to the abovementioned emissions, there are also some minor peaks related to contamination, as shows the comparison between the spectra of the BPT-coated and bare GaAs. The "contamination" contribution can be clearly seen in

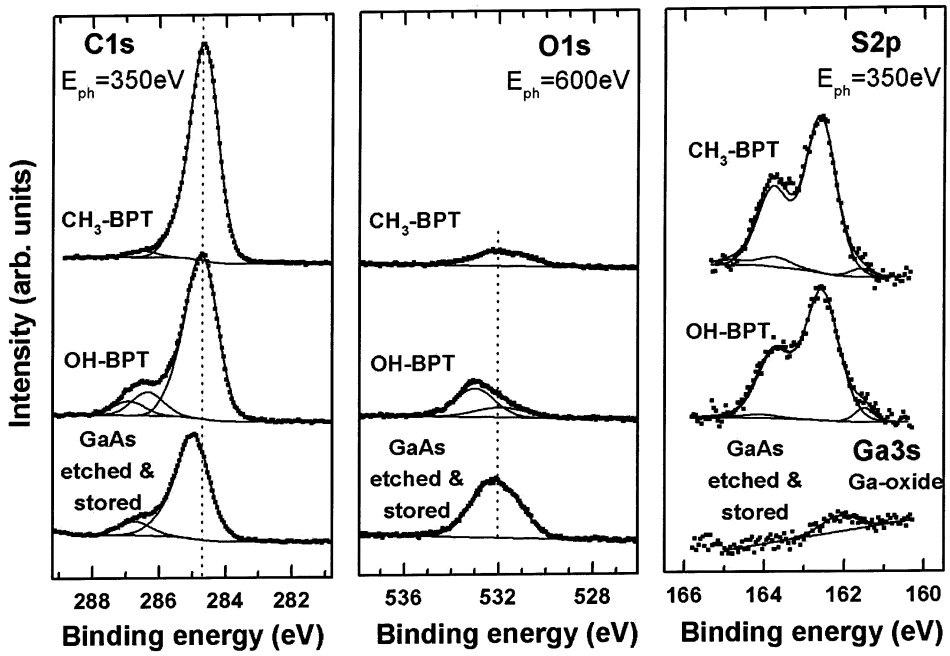

Figure 4. C 1s, O 1s, and S 2p HRXPS spectra of CH_3−BPT- and OH−BPT-coated GaAs as well as the respective spectra of N_2-stored (after the etching) bare GaAs (bottom curves). A decomposition of some spectra by singlets (C 1s and O 1s) or doublets (S 2p) related to the individual chemical species or shake-up excitations is shown (see text for details).

the O 1s spectra, at 532.0 eV, while the respective emission cannot be clearly distinguished in the C 1s spectra. It is, however, clearly seen that the positions of the main C 1s emission for the carbon contamination (bottom spectrum in the left panel in Figure 4) and BPT molecules are noticeably different. Under these circumstances, the presence of a noticeable amount of the contamination in the SAMs will result in an asymmetry of the main C 1s emission. Since such an asymmetry is not observed, one can conclude that the amount of the carbon contamination is rather small.

The total C 1s intensity of the CH_3−BPT-coated GaAs is by about 10% higher than this value for the OH−BPT film. This assumes a higher surface coverage and a higher SAM quality in the CH_3−BPT. This conclusion is in accordance with the Ga 3d and As 3d spectra of the CH_3−BPT- and OH−BPT-coated GaAs (upper panels in Figures 2 and 3), which exhibit a slightly higher extent of the surface oxidation in the OH−BPT.

3.2 NEXAFS Measurements. Normalized C K-edge NEXAFS spectra of CH_3−BPT- and OH−BPT-coated GaAs acquired at X-ray incidence angles of 70°, 55°, and 20° are presented in Figures 5 and 6, respectively, along with the respective difference spectra. The spectra are dominated by an intense π_1* resonance at 285.1 eV, which is characteristic of intact aromatic rings. Along with this resonance, there are other characteristic absorption maxima,[44,45−49] such as R*/C−S* resonance at 287.4 eV,[50−52] a π_2* resonance at 288.6 eV (there is also an alternative σ*(CH) assignment for this resonance),[53,54] and σ* resonances at ≈293.0 eV and ≈302.0 eV. The absorption edge is presumably located at ≈287 eV.[45−47] The π_2* resonance presumably overlaps with a π*-type resonance of residual C═O, which is located at a close photon energy.[29] This is especially pronounced in the OH−BPT-coated GaAs (Figure 6). Also, the height of the π* and R* resonances of the aromatic rings is smaller for this film as compared to that of CH_3−BPT (Figure 5).

As seen in Figures 5 and 6, the intensities of the π* and σ* resonances change when the X-ray incidence angle is varied. This linear dichroism suggests an orientational order in the CH_3−BPT and OH−BPT monolayers on GaAs. Considering that the intensity of the π* resonance increases and that of the σ* resonances decreases with increasing X-ray incidence angle, an upright orientation of the biphenyl moieties can be assumed for both systems. The transition dipole moment (TDM) of the π* resonances is directed perpendicular to the ring plane, whereas the TDM of the σ* resonances is oriented within this plane.

Except for the above qualitative conclusions on the orientational order in the CH_3−BPT and OH−BPT films on GaAs, the average tilt angle of the aromatic chains in these systems can be estimated by a quantitative analysis of the angular dependence of the NEXAFS resonance intensities.[29] For this evaluation, the π_1* resonance has been selected as the most intense absorption feature in the spectra. In addition, this resonance is characteristic for the biphenyl backbone, so that the presence of the carbon contamination did not perturb the estimation of the tilt angle.

For an assumed planar conformation of the biphenyl moieties in the CH_3−BPT- and OH−BPT films (the dihedral angle is equal to zero),[45,55] the average tilt angle φ of the molecular axis of the biphenyl moiety is given by[29,15]

$$I(\theta,\vartheta,\varphi) \propto 1 + (1/2)\cdot(3\cdot\cos^2\theta - 1)\cdot(3\cdot\cos^2\vartheta\cdot\sin^2\varphi - 1) \quad (1)$$

where θ is an X-ray incidence angle and ϑ is the twist angle of the aromatic rings with respect to the plane spanned by the surface normal and the molecular axis. Taking a herringbone arrangement of the BPT molecules such as in the bulk materials and aromatic SAMs on Au,[45,56,57] one finds two possible spatial orientations of the biphenyl moieties with reverse twist angles $\vartheta_1 = -\vartheta_2$, but the same tilt angles $\varphi_1 = \varphi_2$. In this case, the contributions of each spatial orientation to the resonance intensity $I(\theta,\vartheta,\varphi)$ are the same and eq 1 can be used for the data evaluation without any modification. A herringbone structure of the aromatic moieties optimizes the intermolecular interaction in the densely packed 2D-layers.[58,59]

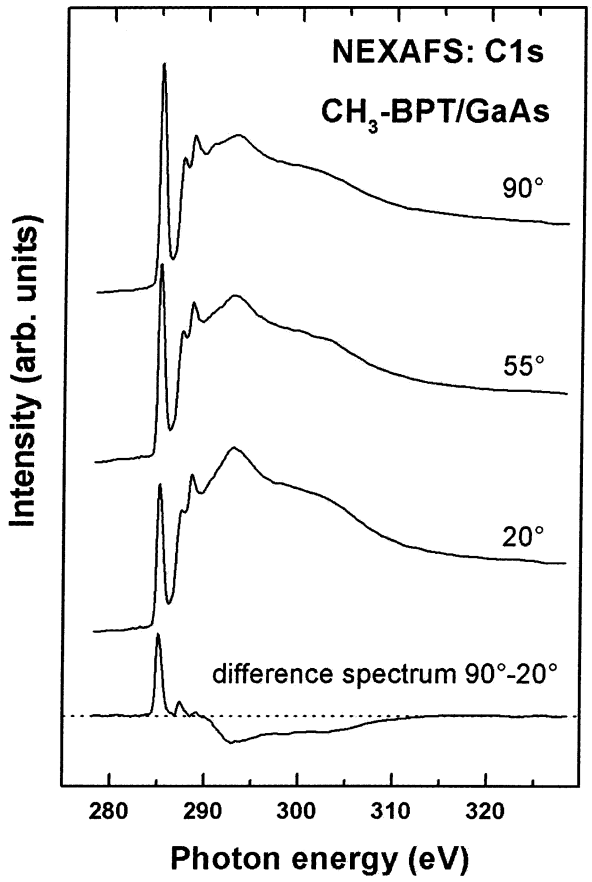

Figure 5. C K-edge NEXAFS spectra of a CH_3−BPT-coated GaAs acquired at X-ray incidence angles of 90°, 55°, and 20° along with the respective difference between the 90° and 20° spectra (bottom curve). The spectra are normalized to the height of the absorption edge.

To avoid normalization problems, not the absolute intensities but the intensity ratios $I(\theta)/I(20°)$ were analyzed.[29] In addition, a twist angle of 32° was assumed, as found for thioaromatic bulk materials.[60−63] This assumption is based on theoretical estimates for the molecular arrangements in biphenyl and naphthalene mercaptan films on Au[56] and on the experimental data for a series of oligo(phenylethynyl)benzenethiols.[57]

The angular dependencies of the π_1* resonance intensity ratio $I(\theta)/I(20°)$ for the CH_3−BPT- and OH−BPT-coated GaAs are presented in Figure 7, together with the best theoretical fits based on expression 1. As is seen in Figure 7, the fits describe the observed experimental dependences rather well. The derived values of the average tilt angles of the biphenyl moieties are given at the respective curves: 31.0° ± 5° and 37.2° ± 5° for GaAs coated with CH_3−BPT and OH−BPT, respectively (the large error bars are mostly related to the uncertainty in the value of the twist angles). These angles are larger than the respective values for BPT SAMs on noble metal substrates (23° for Au and 18° for Ag)[47] but are quite close to the corresponding angles for nonsubstituted BPT SAMs on (100) GaAs (31.5°) and SAMs formed from 4-hydroxy-1,1′-biphenyl (HBP) on hydrogenated Si (111) substrates (28.7°).[49] Similar assumptions concerning the 2D-arrangements of the biphenyl moieties have also been made for BPT on Au,[47] Ag,[47] and GaAs,[15] as well as for HBP on Si,[49] which allows the direct comparison of the derived tilt angles.

Also, the average tilt angle of the biphenyl moieties in the CH_3−BPT film on GaAs is noticeably smaller than that in the OH−BPT SAMs on this substrate, which suggests a higher orientational order in the former layer.

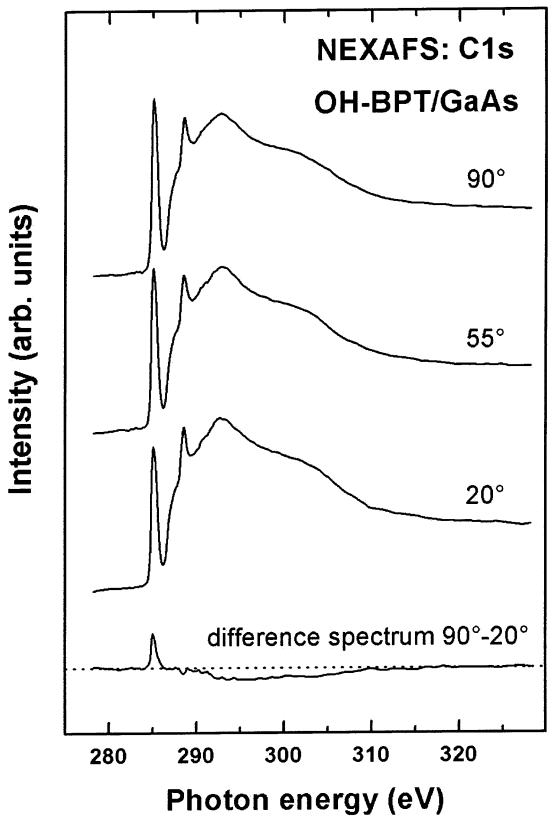

Figure 6. C K-edge NEXAFS spectra of a OH−BPT-coated GaAs acquired at X-ray incidence angles of 90°, 55°, and 20° along with the respective difference between the 90° and 20° spectra (bottom curve). The spectra are normalized to the height of the absorption edge.

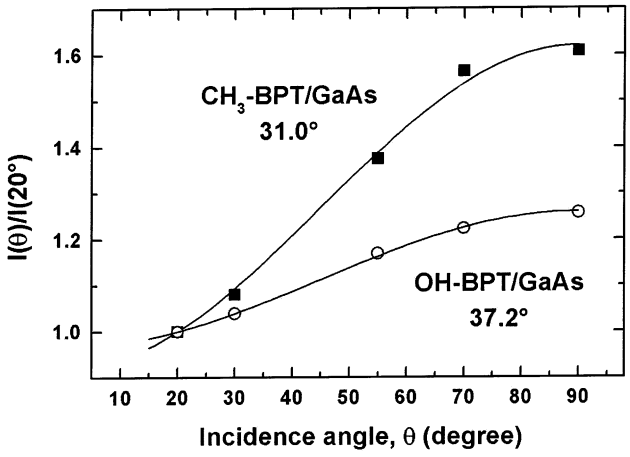

Figure 7. The angular dependencies of the π_1* resonance intensity ratio $I(\theta)/I(20°)$ for CH_3−BPT- and OH−BPT-coated GaAs (quadrates and circles, respectively). The best fits of the experimental data according to eq 1 are marked by the solid line. The derived values of the average tilt angle of the biphenyl backbone are given at the respective curves.

4. Discussion

We demonstrated that both types of 4′-substituted-4-mercaptobiphenyls (CH_3−BPT and OH−BPT) studied here form ordered and densely packed SAMs on GaAs(100) substrates. The covalent attachment to the substrate occurs over the thiolate headgroup, as indicated by the appearance of the respective emissions in the S 2p and As 3d HRXPS spectra. The presence of the entire variety of the characteristic absorption resonances of phenyl rings in the C K-edge NEXAFS spectra suggests the intact character of the biphenyl backbones in both CH_3−BPT

and OH−BPT films. In addition, pronounced linear dichroism implies an orientational order in these films, with an upright orientation of the molecular backbones.

The spectroscopic characterization of several reference samples (bare GaAs) and the SAM/GaAs interface shows that the functionalization of *n*-GaAs with 4′-substituted-4-mercaptobiphenyls prevents an oxidation and contamination of its surface, keeping it in a similar state as the surface of freshly etched GaAs. This is in a full agreement with earlier electrochemical results on stability of the CH_3−BPT- and OH−BPT-coated GaAs in aqueous electrolytes.[17]

Both HRXPS and NEXAFS data suggest that the identity of the functional group affects the quality of the resulting SAMs on the GaAs substrate. The HRXPS spectra of the OH−BPT films imply a slightly higher degree of the surface oxidation and a lower packing density (by ≈10%) as compared to the CH_3−BPT films. Both these conclusions are supported by the NEXAFS data. First, we observed a pronounced signature of the C═O group in the spectrum of OH−BPT-coated GaAs. Second, the height of the π^* resonances is smaller for the OH−BPT film. Third, the quantitative analysis of NEXAFS spectra results in average tilt angles of the biphenyl moieties of 31.0° ± 5° and 37.2° ± 5° for CH_3−BPT and OH−BPT SAMs, respectively. Taking these angles and a length of the BPT molecule of 13.0 Å,[18] one gets effective film thickness of 11.15 Å and 10.35 Å for CH_3−BPT and OH−BPT, respectively, which gives a ≈7.5% lower packing in the latter case, in a good agreement with the HRXPS data.

Comparing the results for the CH_3−BPT and OH−BPT films on GaAs(100) with those for the SAMs of nonsubstituted BPT on the same substrate,[14,15] we can conclude that the nonpolar and weakly interacting CH_3 substitution does not lead to noticeable changes in the packing density and molecular orientation in the film as, for example, follows from comparison of the average tilt angles of the biphenyl moieties in both cases: 31.5° and 31.0° for the BPT and CH_3−BPT SAM, respectively. At the same time, in contrast to the CH_3 group, polar OH substitution causes a partial deterioration of the film quality. On one hand, this can be related to a bonding of hydroxy tailgroups to the highly reactive GaAs surface, which can be followed by molecular decomposition. On the other hand, the deterioration can be caused by a dipole interaction between the hydroxy groups, as this happens for *ω*-substituted *n*-alkanethiols,[64,65] or by the formation of hydrogen bonds between the neighboring molecules at the SAM-ambient interface. In an extreme form, the latter mechanism can even lead to a bilayer formation, as happens in the carboxyl-terminated terphenylthiols on Au.[45]

Even in nonsubstituted or CH_3-substituted BPT, the orientational order in the respective films on GaAs is noticeably lower than that in the analogous thioaromatic SAMs on noble metal substrates (see section 3.2).[45,47] This can be presumably related to the surface contamination at the SAM/GaAs interface—the signature of such a contamination is clearly seen in the As 3d and Ga 3d spectra in Figures 2 and 3. A partial oxidation and the presence of contamination might disturb the anchoring and ordering of the CH_3−BPT and OH−BPT molecules. Improvement in the wet chemical etching or the development of a more sophisticated cleaning procedure (see, e.g., ref 66) might be helpful to remove the residual oxide and other contaminants before the SAM coating. However, the etching procedure applied in this study is the result of a long-time optimization work,[11] including the analysis and repetition of most suitable approaches from the available literature.[4,67−71] Also, a larger lattice spacing between As atoms on GaAs(100) surface (5.6 Å as compared to ≈5.0 Å for (111) Au and Ag)[72] can influence the packing density as well, since a larger separation of the anchor sites generally results in a less dense packing with a larger inclination of the SAM constituents.

A partial inhomogeneity of the SAM/GaAs interface is also exhibited by the S 2p spectra of the CH_3−BPT- and OH−BPT-coated GaAs in Figure 4. The fwhm's of the S $2p_{3/2}$ and S $2p_{1/2}$ components in these spectra (0.93 and 1.0 eV for CH_3−BPT and OH−BPT, respectively) are noticeably larger than the analogous value for a structurally and chemically homogeneous 2D-array of the thiolate headgroups (0.50 eV)[28] or even that for the thiolate headgroups in AT/Au (0.56 eV)[26] or BPT/Au (0.50−0.73 eV).[26] This suggests a distribution of different bonding geometries or local atomic arrangements at the SAM/GaAs interface, resulting in slightly shifted emission peaks, which all together produce a broad spectral feature.

Apart from the above-discussed fwhm of the S 2p components, the BE position of the S 2p doublet in the respective spectra of the CH_3−BPT- and OH−BPT-coated GaAs is of a special interest, as already mentioned in section 3.1. The respective value of 162.6 eV (S $2p_{3/2}$) is somewhat higher than the 162.0 eV observed for the thiol-derived SAMs on noble metal substrates.[26,42−44] Assuming that the difference is predominantly related to the screening of the photoemission hole by the substrate electrons in the metal substrates and taking into account the BE position of the unbound thiol (163.3 eV for S $2p_{3/2}$),[21] we can untangle the "bonding" and "screening" contributions in the S 2p photoemission of thiol-derived SAMs. The screening of the photoemission hole by the substrate electrons of the metal substrates can then be estimated as ≈0.6 eV (a BE shift) while the charge transfer upon the formation of the thiolate bond results in a BE shift of ≈0.7 eV.

5. Conclusions

Using HRXPS and NEXAFS spectroscopy, we demonstrated that 4′-substituted-4-mercaptobiphenyls CH_3−BPT and OH−BPT form ordered and densely packed SAMs on GaAs(100) substrates. The covalent coupling of BPT derivatives enables both the protection of the GaAs surface from degradation and the control over the surface free energy of the engineered GaAs. Such a functionalization protocol can be used to optimize the interface matching to polymer films and model biomembranes.[73−76] It can also be directly transferred onto various semiconductor heterostructures in the proximity of the GaAs surface, such as near-surface quantum dots[12,13] or 2D electron gas assembly,[16] which allow for sensitive detection of specific recognition and selective transport in biological membranes.

The attachment of the CH_3−BPT and OH−BPT molecules to the GaAs substrate is mediated by the As-thiolate bond while the intact aromatic backbones have an upright orientation with average tilt angles of 31.0° ± 5° and 37.2° ± 5° for CH_3−BPT and OH−BPT films, respectively. Accordingly, the packing density of the former SAM is by 7−10% higher than that of the latter one. The results suggest that nonpolar and weakly interacting substitutions do not lead to noticeable changes in the packing density and molecular orientation in the BPT film on GaAs, whereas a polar and chemically active substitution may cause a partial deterioration of the film quality.

Even for nonsubstituted or CH_3-substituted BPT, the orientational order and structural homogeneity in the respective films on GaAs is noticeably lower than that in the analogous thioaromatic SAMs on noble metal substrates, which can be attributed to the large spacing between the surface arsenides

(5.6 Å) or the presence of residual contamination and oxides on the surface of the GaAs substrate. The contaminants are associated with a high chemical reactivity of a bare GaAs surface and a basic constrain of the etching procedure, performed under ambient, even though with a N_2 protection.

As a side result, we succeeded to untangle the bonding and screening contributions in the S 2p photoemission of thiol-derived SAMs. The BE shifts due to the screening of the photoemission hole by the substrate electrons of the metal substrate and due to the formation of the thiolate bond were estimated as ≈0.6 eV and ≈0.7 eV, respectively.

Finally, we would like to emphasize that synchrotron-based HRXPS and NEXAFS spectroscopy applied in this study are well suited for quantitative characterization of complex multi-component systems. An ultimate energy resolution of HRXPS and tunability of the synchrotron radiation are important advantages, allowing one to probe different regions within the samples and to avoid a standard problem of arbitrary decomposition of broad emission features.

Acknowledgment. We thank the BESSY II and MAX-lab staff for technical help and Ch. Wöll (Universität Bochum) for providing us with experimental equipment for the NEXAFS measurements. We are very grateful to M. Bichler, D. Schuh, M. Tornow, and G. Abstreiter (Walter Schottky Institute, TUM) for providing MBE-grown GaAs wafers and E. Sackmann for helpful discussion. This work has been supported by the German BMBF (GRE1HD and 05KS4VHA/4), the Deutsche Forschungsgemeinschaft (SFB563, Ta259/1), Access to Research Infrastructure action of the Human Potential Programme of the European Community, and by the Fonds der Chemischen Industrie. M. T. is a recipient of Emmy Noether fellowship of DFG.

References and Notes

(1) Baumgartner, P.; Engel, C.; Abstreiter, G.; Böhm, G.; Weimann, G. *Appl. Phys. Lett.* **1994**, *64*, 592.
(2) Baumgartner, P.; Engel, C.; Abstreiter, G.; Böhm, G.; Weimann, G. *Appl. Phys. Lett.* **1995**, *66*, 751.
(3) Ulman, A. *Chem. Rev.* **1996**, *96*, 1533.
(4) Sheen, C. W.; Shi, J.-X.; Martensson, J.; Parikh, A. N.; Allara, D. L. *J. Am. Chem. Soc.* **1992**, *114*, 1514.
(5) Lercel, M. J.; Redinbo, G. F.; Pardo, F. D.; Rooks, M.; Tiberio, R. C.; Simpson, P.; Craighead, H. G.; Sheen, C. W.; Parikh, A. N.; Allara, D. L. *J. Vac. Sci. Technol., B* **1994**, *12*, 3663.
(6) Dorsten, J. F.; Maslar, J. E.; Bohn, P. W. *Appl. Phys. Lett.* **1995**, *66*, 1755.
(7) Onho, H.; Motomatsu, M.; Mizutani, W.; Tokumoto, H. *Jpn. J. Appl. Phys.* **1995**, *34*, 1381.
(8) Lercel, M. J.; Craighead, H. G.; Parikh, A. N.; Seshadri, K.; Allara, D. L. *J. Vac. Sci. Technol., A* **1996**, *14*, 1844.
(9) Seshadri, K.; Froyd, K.; Parikh, A. N.; Allara, D. L.; Lercel, M. J.; Craighead, H. G. *J. Phys. Chem.* **1996**, *100*, 15900.
(10) Adlkofer, K.; Tanaka, M.; Hillebrandt, H.; Wiegand, G.; Sackmann, E.; Bolom, T.; Deutschmann, R.; Abstreiter, G. *Appl. Phys. Lett.* **2000**, *76*, 3313.
(11) Adlkofer, K.; Tanaka, M. *Langmuir* **2001**, *17*, 4267.
(12) Duijs, E. F.; Findeis, F.; Deutschmann, R. A.; Bichler, M.; Zrenner, A.; Abstreiter, G.; Adlkofer, A.; Tanaka, M.; Sackmann, E. *Phys. Status Solidi B* **2001**, *224*, 871.
(13) Adlkofer, K.; Duijs, E. F.; Findeis, F.; Bichler, M.; Zrenner, A.; Sackmann, E.; Abstreiter, G.; Tanaka, M. *Phys. Chem. Chem. Phys.* **2002**, *4*, 785.
(14) Adlkofer, K.; Eck, W.; Grunze, M.; Tanaka, M. *J. Phys. Chem. B* **2003**, *107*, 587.
(15) Shaporenko, A.; Adlkofer, K.; Johansson, L. S. O.; Tanaka, M.; Zharnikov, M. *Langmuir* **2003**, *19*, 4992.
(16) Luber, S.; Adlkofer, A.; Rant, U.; Ulman, A.; Gölzhäuser, A.; Grunze, M.; Schuh, D.; Tanaka, M.; Tornow, M.; Abstreiter, G. *Physica E* **2004**, *21*, 1111.
(17) Adlkofer, K.; Shaporenko, A.; Zharnikov, M.; Grunze, M.; Ulman, A.; Tanaka M. *J. Phys. Chem. B* **2003**, *107*, 11737.
(18) Kang, J. F.; Jordan, R.; Ulman, A. *Langmuir* **1998**, *14*, 3983.
(19) Wirde, M.; Gelius, U.; Dunbar, T.; Allara, D. L. *Nucl. Instrum. Methods Phys. Res., B* **1997**, *131*, 245.
(20) Jäger, B.; Schürmann, H.; Müller, H. U.; Himmel, H.-J.; Neumann, M.; Grunze, M.; Wöll, Ch. *Z. Phys. Chem.* **1997**, *202*, 263.
(21) Heister, K.; Zharnikov, M.; Grunze, M.; Johansson, L. S. O.; Ulman, A. *Langmuir* **2001**, *17*, 8.
(22) Zharnikov, M.; Grunze, M. *J. Vac. Sci. Technol., B* **2002**, *20*, 1793.
(23) Band, I. M.; Kharitonov, Yu. I.; Trzhaskovskaya, M. B. *At. Data Nucl. Data Tables* **1979**, 23, 443.
(24) Goldberg, S. M.; Fadley, C. S.; Kono, S. *J. Electron Spectrosc. Relat. Phenom.* **1981**, *21*, 285.
(25) Yeh, J. J.; Lindau, I. *At. Data Nucl. Data Tables* **1985**, *32* 1.
(26) Heister, K.; Zharnikov, M.; Grunze, M.; Johansson, L. S. O. *J. Phys. Chem. B* **2001**, *105*, 4058.
(27) *Surface chemical analysis − X-ray photoelectron spectrometers − Calibration of energy scales*, ISO 15472: 2001.
(28) Heister, K.; Rong, H.-T.; Buck, M.; Zharnikov, M.; Grunze, M.; Johansson, L. S. O. *J. Phys. Chem. B* **2001**, *105*, 6888.
(29) Stöhr, J. *NEXAFS Spectroscopy*; Springer Series in Surface Science 25; Springer-Verlag: Berlin, 1992.
(30) Frey, S.; Heister, K.; Zharnikov, M.; Grunze, M., Tamada, K.; Colorado, R., Jr.; Graupe, M.; Shmakova, O. E.; Lee, T. R. *Isr. J. Chem.* **2000**, *40*, 81.
(31) Zharnikov, M.; Frey, S.; Heister, K.; Grunze, M. *Langmuir* **2000**, *16*, 2697.
(32) Batson, P. E. *Phys. Rev. B* **1993**, *48*, 2608.
(33) Lindau, I.; Spicer, W. E. *J. Electron Spectrosc.* **1974**, *3*, 409.
(34) Powell, C. J. *Surf. Sci.* **1974**, *44*, 29.
(35) Chang, S.; Vitomirov, I. M.; Brillson, L. J.; Rioux, D. F.; Kirchner, P. D.; Pettit, G. D.; Woodall, J. M. *J. Vac. Sci. Technol., B* **1991**, *9*, 2129.
(36) Wagner, C. D.; Riggs, W. M.; Davis, L. E.; Moulder, J. F.; Muilenberg, J. E. *Handbook of X-ray Photoelectron Spectroscopy*; Perkin-Elmer Corp.: Eden Prairie, MN, 1979.
(37) Mao, D.; Kahn, A.; Le Lay, G.; Marsi, M.; Hwu, Y.; Margaritondo, G.; Santos, M.; Shayegan, M.; Florez, L. T.; Harbison, J. P. *J. Vac. Sci. Technol., B* **1991**, *9*, 2083.
(38) Lunt, S. R.; Ryba, G. N.; Santangelo, P. G.; Lewis, N. S. *J. Appl. Phys.* **1991**, *70*, 7449.
(39) Lunt, S. R.; Santangelo, P. G.; Lewis, N. S *J. Vac. Sci. Technol., B* **1991**, *9*, 2333.
(40) Shin, J.; Geib, K. M.; Wilmsen, C. W. *J. Vac. Sci. Technol., B* **1991**, *9*, 2337.
(41) Moulder, J. F.; Stickle, W. E.; Sobol, P. E.; Bomben, K. D. *Handbook of X-ray Photoelectron Spectroscopy*; Chastian, J., Ed.; Perkin-Elmer Corp.: Eden Prairie, MN, 1992.
(42) Laibinis, P. E.; Whitesides, G. M.; Allara, D. L.; Tao, Y.-T.; Parikh, A. N.; Nuzzo, R. G. *J. Am. Chem. Soc.* **1991**, *113*, 7152.
(43) Himmelhaus, M.; Gauss, I.; Buck, M.; Eisert, F.; Wöll, Ch.; Grunze, M. *J. Electron Spectrosc. Relat. Phenom.* **1998**, *92*, 139.
(44) Zharnikov, M.; Grunze, M. *J. Phys.: Condens. Matter* **2001**, *13*, 11333.
(45) Himmel, H.-J.; Terfort, A.; Wöll, Ch. *J. Am. Chem. Soc.* **1998**, *120*, 12069.
(46) Geyer, W.; Stadler, V.; Eck, W.; Zharnikov, M.; Gölzhäuser, A.; Grunze, M. *Appl. Phys. Lett.* **1999**, *75*, 2401.
(47) Frey, S.; Stadler, V.; Heister, K.; Zharnikov, M.; Grunze, M.; Zeysing, B.; Terfort, A. *Langmuir* **2001**, *17*, 2408.
(48) Fuxen, C.; Azzam, W.; Arnold, R.; Witte, G.; Terfort, A.; Wöll, Ch. *Langmuir* **2001**, *17*, 3689.
(49) Zharnikov, M.; Küller, A.; Shaporenko, A.; Schmidt, E.; Eck, W. *Langmuir* **2003**, *19*, 4682.
(50) Horsley, J. A.; Stöhr, J.; Hitchcock, A. P.; Newbury, D. C.; Johnson, A. L.; Sette, F. *J. Chem. Phys.* **1985**, *83*, 6099.
(51) Stöhr, J.; Outka, D. A. *Phys. Rev. B* **1987**, *36*, 7891.
(52) Weiss, K.; Gebert, S.; Wühn, M.; Wadepohl, H.; Wöll, Ch. *J. Vac. Sci. Technol., A* **1998**, *16*, 1017.
(53) Yokoyama, T.; Seki, K.; Morisada, I.; Edamatsu, K.; Ohta, T. *Phys. Scr.* **1990**, *41*, 189.
(54) Ågren, H.; Vahtras, O.; Carravetta, V. *Chem. Phys.* **1995**, *196*, 47.
(55) Lii, J.-H.; Allinger, N. L. *J. Am. Chem. Soc.* **1989**, *111*, 8576.
(56) Chang, S.-C.; Chao, I.; Tao, Y.-T. *J. Am. Chem. Soc.* **1994**, *116*, 6792.
(57) Dhirani, A.-A.; Zehner, W.; Hsung, R. P.; Guyot-Sionnest, P.; Sita, L. *J. Am. Chem. Soc.* **1996**, *118*, 3319.
(58) Sabatani, E.; Cohen-Boulakia, J.; Bruening, M.; Rubinstein, I. *Langmuir* **1993**, *9*, 2974.
(59) Ulman, A. *Acc. Chem. Res.* **2001**, *34*, 855.
(60) Cruickshank, D. W. J. *Acta Crystallogr.* **1956**, *9*, 915.
(61) Kitaigorodskii, I. A. *Organic Chemical Crystallography*; Consultants Bureau: New York, 1961.
(62) Trotter, J. *Acta Crystallogr.* **1961**, *14*, 1135.
(63) Charbonneau, G.-P.; Delugeard, Y. *Acta Crystallogr.* **1976**, *B32*, 1420.

(64) Dannenberger, O.; Weiss, K.; Himmel, H.-J.; Jäger, B.; Buck, M.; Wöll, Ch. *Thin Solid Films* **1997**, *307*, 183.
(65) Frey, S.; Shaporenko, A.; Zharnikov, M.; Harder, P.; Allara, D. L. *J. Phys. Chem. B* **2003**, *107*, 7716.
(66) Razek, N.; Otte, K.; Chasse, T.; Hirsch, D.; Schindler, A.; Frost, F.; Rauschenbach, B. *J. Vac. Sci. Technol., A* **2002**, *20*, 1492.
(67) Vasquez, R. P.; Lewis, B. F.; Grunthar, F. J. *J. Vac. Sci. Technol.* **1983**, *B1*, 791.
(68) Woodall, J. M.; Oelhafen, P.; Jackson, T. N.; Freeouf, J. L.; Pettit, G. D. *J. Vac. Sci. Technol.* **1983**, *B*1, 795.
(69) Sze, S. M. *Semiconductor Devices: Physics and Technology*; John Wiley & Sons: New York, 1985.
(70) Lunt, S. R.; Ryba, G. N.; Santangelo, P. G.; Lewis, N. S. *J. Appl. Phys.* **1991**, *70*, 7449.
(71) Nakagawa, O. S.; Ashok, S.; Sheen, C. W.; Martensson, J.; Allara, D. L. *Jpn. J. Appl. Phys.* **1991**, *30*, 3759.
(72) Bain, C. D. *Adv. Mater.* **1992**, *4*, 591.
(73) Sackmann, E.; Tanaka, M. *Trends Biotechnol.* **2000**, *18*, 58.
(74) Hillebrandt, H.; Wiegand, G.; Tanaka, M.; Sackmann, E. *Langmuir* **1999**, *15*, 8451.
(75) Tanaka, M.; Kaufmann, S.; Nissen, J.; Hochrein, M. *Phys. Chem. Chem. Phys.* **2001**, *3*, 4091.
(76) Hillebrandt, H.; Tanaka, M.; Sackmann, E. *J. Phys. Chem. B* **2002**, *106*, 477.